Surface acoustic-wave attenuation by a two-dimensional electron gas in a strong magnetic field

Andreas Knäbchen and Yehoshua B. Levinson
Weizmann Institute of Science, Department of Condensed Matter Physics, 76100 Rehovot, Israel

Ora Entin-Wohlman
School of Physics and Astronomy, Raymond and Beverly Sackler Faculty of Exact Sciences, Tel Aviv University, 69978 Tel Aviv, Israel

(Received 29 January 1996)

The propagation of a surface acoustic wave (SAW) on GaAs/Al_xGa_{1-x}As heterostructures is studied in the case where a two-dimensional electron gas (2DEG) is subject to a strong magnetic field and a smooth random potential with correlation length Λ and amplitude Δ. The electron wave functions are described in a quasiclassical picture using results of percolation theory for two-dimensional systems. In accordance with the experimental situation, Λ is assumed to be much smaller than the sound wavelength $2\pi/q$. This restricts the absorption of surface phonons at a filling factor $\overline{\nu}\approx\frac{1}{2}$ to electrons occupying extended trajectories of fractal structure. Both piezoelectric and deformation potential interactions of surface acoustic phonons with electrons are considered and the corresponding interaction vertices are derived. These vertices are found to differ from those valid for three-dimensional bulk phonon systems with respect to the phonon wave-vector dependence. We derive the appropriate dielectric function $\varepsilon(\omega,q)$ to describe the effect of screening on the electron-phonon coupling. In the low-temperature, high-frequency regime $T\ll\Delta(\omega_q\Lambda/v_D)^{\alpha/2\nu}$, where ω_q is the SAW frequency and v_D is the electron drift velocity, both the attenuation coefficient Γ and $\varepsilon(\omega,q)$ are independent of temperature. The classical percolation indices give $\alpha/2\nu=3/7$. The width of the region where a strong absorption of the SAW occurs is found to be given by the scaling law $|\Delta\overline{\nu}|\approx(\omega_q\Lambda/v_D)^{\alpha/2\nu}$. The dependence of the electron-phonon coupling and the screening due to the 2DEG on the filling factor leads to a double-peak structure for $\Gamma(\overline{\nu})$. [S0163-1829(96)06739-2]

I. INTRODUCTION

Surface acoustic waves (SAW's) (Refs. 1 and 2) provide a useful tool for experimental studies of the two-dimensional electron gas (2DEG) in GaAs/Al_xGa_{1-x}As heterostructures. In particular, SAW's have been used in recent years in investigations of the integer[3–7] and the fractional[7–9] quantum Hall regimes. Due to the quantum Hall effect, the interaction of the SAW with the charge carriers can lead to strong oscillations in the attenuation and the velocity of the sound waves as function of the applied magnetic field. Quantum oscillations have also been reported for the sound-induced currents and voltages.[7,10]

Previous theoretical descriptions of these experiments have been based essentially on classical models for the propagation of SAW's.[11,12] According to these models, which are originally derived for systems in the absence of an applied magnetic field, the sound attenuation is expressed in terms of the electrical dc conductivity. This relation is derived under the assumptions that $ql\ll1$ and $\omega_q\tau\ll1$ (local regime), where $\boldsymbol{q}$ and ω_q are the wave vector and the frequency of the sound, respectively, and l and τ are the mean free path and the scattering time of the conduction electrons, respectively. If a (classical) magnetic field is applied, the first condition has to be replaced by $qR_c\ll1$, where R_c is the cyclotron radius.[12] It is much more difficult, however, to determine under which conditions the above-mentioned theories are valid when the 2DEG is subject to a quantizing magnetic field. In this case, the electron system is characterized by (at least) two more length scales, namely, the magnetic length $l_B=\sqrt{c\hbar/eB}$ and the localization length[13] ξ. While $ql_B\ll1$ is always fulfilled under typical experimental conditions, the localization length can be much larger than the surface acoustic wavelength $2\pi/q$.

A series of experiments[3–9] has shown a reasonable agreement with the predictions of classical models in a wide range of frequencies ω_q and magnetic-field strengths. On the other hand, some deviations have also been detected. For example, deviations of the SAW attenuation from classically predicted behavior with increasing frequency have been reported.[5] These were attributed to nonlocal effects of the interaction between the SAW and the 2DEG which should occur when the sound wavelength becomes of the order of or smaller than a characteristic length scale of the electron gas. In the fractional quantum Hall regime, an anomaly in the absorption coefficient for filling factor $\overline{\nu}=\frac{1}{2}$ was found.[8,9] This anomaly was discussed in the framework of the composite fermion model of Ref. 14. According to this approach, electrons are replaced by composite fermions moving in an effective magnetic field of zero average (at $\overline{\nu}=\frac{1}{2}$). Then the sound absorption due to these particles is described by classical formulas, except that the dc conductivity is replaced by the wave-vector-dependent nonlocal conductivity which, however, represents a very important difference (see Ref. 14 for details).

In this paper we study the propagation of SAW's in the integer quantum Hall regime. The calculation of the SAW attenuation is carried out for filling factors near $\frac{1}{2}$, and is based on a percolation approach to the electronic states in a very strong magnetic field. From this point of view we may

anticipate a nonlocal behavior of the attenuation arising from large characteristic length scales (e.g., the size of a percolation cluster $\gg q^{-1}$) inherent in that framework. The effect of electron-electron interaction is taken into account by the screening of the electron-phonon coupling. The same problem has also been studied in Ref. 15. These authors calculated the nonlocal conductivity due to variable-range hopping between pairs of localized states. Then, in the spirit of the classical description of sound absorption, this conductivity is related to the SAW attenuation coefficient. A comparison with our results will be given in Sec. VI.

The system considered is a 2DEG, subject to a very strong magnetic field B and a smooth random potential V. The potential can be characterized by its amplitude Δ and its correlation length Λ. The amplitude also determines the width of the Landau levels. The correlation length is of the order of the spacer layer that separates the 2DEG from the dopant layers. Under the assumption that $l_B \ll \Lambda$ is a quasiclassical description of the electron states can be applied. That is, one considers the drift motion of the guiding center of an electron on the equipotential lines (EL's) of V separately from the rapid motion relative to it.[13] The drift velocity is given by $v_D = c|\nabla V|/eB$. Using $|\nabla V| \simeq \Delta/\Lambda$, the drift velocity can be estimated to be $v_D \simeq l_B^2 \Delta/\hbar\Lambda$. Depending on the ratio between the correlation length Λ and the sound wavelength, two regimes can be distinguished. For $q\Lambda \gg 1$, the electron-phonon interaction can be considered locally neglecting the global structure of the EL's.[16,17] (For single-phonon absorption and emission processes to occur, one has also to require that the sound velocity v_s is smaller than the drift velocity. This is usually referred to as the Čerenkov condition.[18]) This regime is valid for, e.g., thermal phonons.[16] However, SAW's have a much larger wavelength, and hence $q\Lambda \ll 1$ is typically fulfilled. In this case, the local absorption and emission of phonons is exponentially small, and the EL as a whole has to be considered. It becomes important that the motion of the guiding center on an extended EL (with a length $\gg \Lambda$) resembles a random walk, with a diffusion coefficient $D = v_D \Lambda$. Since the ratio v_D/v_s, for real systems, is not very different from unity, one deals with the limit $\omega_q \gg Dq^2$ of this diffusion process. [To be precise,[18] the parameter v_D/v_s has to lie in the range $q\Lambda \ll v_D/v_s \ll (q\Lambda)^{-3/4}$.] Indeed, for $B = 10$ T ($l_B = 8$ nm), $\Delta = 1$ meV, $\Lambda \approx 50$ nm, $q = 10^4$ cm^{-1}, and $v_s \approx 3 \times 10^5$ cm s^{-1} we find $q\Lambda = 0.05$ and $v_D \approx 0.7 v_s$. It is this particular (diffusive) regime which will be addressed in this paper. In the same regime, the electron lifetime and the energy relaxation time due to interaction with 3D bulk phonons have been calculated in Ref. 18.

The quantum-mechanical calculation of the attenuation coefficient (as well as of other quantities associated with SAW's) requires a knowledge of the Hamiltonians which describe the interaction of electrons with acoustic surface phonons. As far as we know these interaction Hamiltonians have not yet been derived. Instead, many theoretical investigations have addressed the interaction of 2D electrons with 3D (bulk) or 2D phonon systems. The latter one, a single layer of vibrating atoms, represents merely a theoretical construction. Three-dimensional phonons do not provide an appropriate approach when the 2DEG is located near a free-crystal surface.[19] This implies that it is by no means clear that the interaction of a SAW with the 2DEG is described well by the formulas which are valid in the case of bulk phonons. In fact, we find that the interaction vertices appearing in the general electron-phonon interaction Hamiltonian [see Eq. (11)] differ from those for 3D phonons not only by numerical constants but also in the phonon wave-vector dependence and the relative phase between the deformation potential and the piezoelectric interactions.

The paper is organized as follows. The interaction vertices are derived and discussed in Sec. II. In Sec. III, we describe the quasiclassical electron states of a 2DEG in a strong magnetic field and a random potential V. We show that the absorption of the SAW and the dielectric function depend crucially on the occupation and the properties of electron states which correspond to very long EL's. The structure of these EL's is deduced from 2D percolation theory. The matrix elements for transitions between different electron states are given in Sec. IV. The screening of the electron-phonon interaction due to the 2DEG is accounted for by a dielectric function $\varepsilon(\omega_q, q)$ which is calculated in Sec. V. Based on these results, the SAW attenuation coefficient is obtained in Sec. VI. Its dependence on the filling factor (or the Fermi energy), the SAW frequency, and the temperature are discussed. A short summary is given in Sec. VII.

II. INTERACTION HAMILTONIANS

A. Displacement field

To simplify the calculations we use the following assumptions. Since the SAW wavelength $2\pi/q$ is much longer than the lattice constant, the crystal can be approximated by a continuous medium. Its elastic properties are assumed to be isotropic. Furthermore, we disregard the fact that the GaAs substrate is coated with layers which differ slightly in their elastic properties. The overall thickness of these layers[5] $d \simeq 100$ nm is much smaller than the wavelength of sound. It has been shown[2] that for $qd \ll 1$ the deviations of the wave propagation resulting from a thin overlayer coating an homogeneous substrate can be accounted for by a systematic expansion in this small parameter. In our case $qd \leqslant 10^{-1}$, i.e., these corrections are indeed negligible. Thus we end up with the standard problem of sound waves which are propagated in an isotropic medium bounded by a plane.[20,2] (Effects resulting from the anisotropy of the lattice become important for $qd \approx 1$; see Ref. 21.)

Let the surface be in the x-y plane and the medium in the half-space $z \geqslant 0$. The longitudinal and transversal components of the displacement field $\boldsymbol{u}(\boldsymbol{r},t)$, $\boldsymbol{r} = (x,y,z) \equiv (\boldsymbol{R},z)$ obey the wave equations

$$\frac{\partial^2 \boldsymbol{u}_{l,t}}{\partial t^2} - c_{l,t}^2 \Delta \boldsymbol{u}_{l,t} = 0, \tag{1}$$

where $c_{l,t}$ are the corresponding sound velocities. By definition, $\mathrm{curl}\,\boldsymbol{u}_l = 0$ and $\mathrm{div}\,\boldsymbol{u}_t = 0$. Surface waves are composed of particular solutions of Eqs. (1) that decay exponentially with increasing distance from the surface. In addition, these solutions have to satisfy the boundary conditions at the free surface $z = 0$, namely, the normal components of the stress tensor should vanish there. It turns out that these boundary

conditions can only be fulfilled by a linear combination of $\boldsymbol{u}_l$ and $\boldsymbol{u}_t$, i.e., pure longitudinal or transversal surface waves do not exist.[20] The full displacement field for a mode with a two-dimensional wave vector $\boldsymbol{q}$ can be written as

$$\boldsymbol{u}_{\boldsymbol{q}}(\boldsymbol{r},t)=C_q e^{i(\boldsymbol{q}\cdot\boldsymbol{R}-\omega_q t)}\boldsymbol{v}_{\boldsymbol{q}}(z)+\text{c.c.}, \tag{2a}$$

with

$$\boldsymbol{v}_{\boldsymbol{q}}(z)=-i\hat{\boldsymbol{q}}(e^{-\kappa_l qz}-f\kappa_t e^{-\kappa_t qz})+\hat{\boldsymbol{z}}(\kappa_l e^{-\kappa_l qz}-f e^{-\kappa_t qz}). \tag{2b}$$

That is, the displacement $\boldsymbol{u}_{\boldsymbol{q}}$ is polarized in the sagittal plane which is spanned by the propagation direction $\hat{\boldsymbol{q}}=\boldsymbol{q}/q$ and the surface normal $\hat{\boldsymbol{z}}$. The decay of the displacements into the interior of the medium is described by

$$\kappa_l(\alpha)=\sqrt{1-\alpha\xi^2}\ \text{ and }\ \kappa_t(\alpha)=\sqrt{1-\xi^2}, \tag{3}$$

where $\alpha=c_t^2/c_l^2$, and ξ is a root of an algebraic equation of sixth order containing the parameter α only (see Ref. 20). ξ enters the dispersion relation of the surface waves in the form

$$\omega_q=\xi c_t q\equiv v_s q, \tag{4}$$

where v_s is the SAW velocity. Finally, the factor f is given by

$$f(\alpha)=\frac{1+\kappa_t^2}{2\kappa_t}=\left(\frac{\kappa_l}{\kappa_t}\right)^{1/2}. \tag{5}$$

In order to quantize the displacement field (2), the normalization constant C_q of each individual mode has first to be fixed in an appropriate way. That is, the energy associated with the mode $\boldsymbol{u}_{\boldsymbol{q}}(\boldsymbol{r},t)$ in the normalization volume has to coincide with the energy $\hbar\omega_q$ of the corresponding phonon. Since the wave is propagated freely along the surface, the energy is normalized with respect to a large but finite square of area L^2 in the x-y plane. Conversely, no such restriction is necessary with respect to the z coordinate because $\boldsymbol{u}_{\boldsymbol{q}}$ decays exponentially with increasing distance from the surface. Thus the normalization volume can be extended from $z=0$ to $z=\infty$ under the chosen surface area.

Adding a kinetic-energy term to the potential energy[20] associated with a displacement field $\boldsymbol{u}$, the total energy can be written as

$$E(\boldsymbol{u})=\tfrac{1}{2}\rho\int d^3r\Big[(\partial\boldsymbol{u}/\partial t)^2+(c_l^2-2c_t^2)(\text{div}\boldsymbol{u})^2 +2c_t^2\sum_{i,k}(u_{ik})^2\Big], \tag{6}$$

where ρ is the mass density of the medium, and

$$u_{ik}=\frac{1}{2}\left(\frac{\partial u_i}{\partial x_k}+\frac{\partial u_k}{\partial x_i}\right),\quad i,k=x,y,z \tag{7}$$

is the strain tensor. Inserting $\boldsymbol{u}_{\boldsymbol{q}}$, Eq. (2), into this formula, and imposing the condition $E(\boldsymbol{u}_{\boldsymbol{q}})=\hbar\omega_q$ determines the normalization as

$$C_q\equiv C=\frac{1}{L}\left(\frac{\hbar}{\rho v_s a}\right)^{1/2}, \tag{8a}$$

with a numerical factor

$$a(\alpha)=f^3-2f+\frac{1}{\kappa_l}-\frac{\alpha^2\xi^2}{\kappa_l} +\frac{1}{\xi^2}\left[\frac{(1+\kappa_l^2)^2}{2\kappa_l}+\kappa_l(1+f^2)-2f(1+\kappa_l\kappa_t)\right]. \tag{8b}$$

Equations (8) show that the normalization leads merely to a constant prefactor; i.e., in contrast to the case of bulk phonons, C does not introduce a further dependence on the wave number q.

We are now in a position to quantize the displacement field $\boldsymbol{u}_{\boldsymbol{q}}$ [Eqs. (2)] of a SAW. According to the familiar rules, we define the phonon annihilation and creation operators $b_{\boldsymbol{q}}$ and $b_{\boldsymbol{q}}^\dagger$ and for the complete wave field find the expression

$$\boldsymbol{u}(\boldsymbol{r},t)=C\sum_{\boldsymbol{q}}\ [b_{\boldsymbol{q}}e^{i(\boldsymbol{q}\cdot\boldsymbol{R}-\omega_q t)}\boldsymbol{v}_{\boldsymbol{q}}(z)+\text{H.c.}]. \tag{9}$$

B. Deformation-potential interaction

The deformation potential is proportional to the change in volume, div$\boldsymbol{u}$, which an infinitesimal volume element undergoes due to the wave.[22] Introducing an electron-phonon interaction constant Ξ, the Hamiltonian of the deformation potential can be written as

$$H_{DA}=\Xi\,\text{div}\boldsymbol{u}(\boldsymbol{r},t). \tag{10}$$

The spread of the transversal component of the electron wave function as well as the distance d of the 2DEG from the surface are small compared to q^{-1}. Thus, in evaluating Eq. (10), one can set all exponentials in $\boldsymbol{v}_{\boldsymbol{q}}(z)$, Eq. (2b), equal to 1.

Conveniently, the electron-phonon interaction Hamiltonian can be written in the general form

$$H=\frac{1}{L}\sum_{\boldsymbol{q}}\ \gamma_{\boldsymbol{q}}e^{i\boldsymbol{q}\cdot\boldsymbol{R}}b_{\boldsymbol{q}}+\text{H.c.} \tag{11}$$

For a deformation potential interaction, from Eqs. (9) and (10) we derive the interaction vertex

$$\gamma_{\boldsymbol{q}}^{DA}=\left(\frac{\hbar}{\rho v_s a}\right)^{1/2}\alpha\xi^2\Xi q. \tag{12}$$

Following a notation introduced in Ref. 22, the electron-phonon interaction constant Ξ can be replaced by a nominal scattering time τ_{DA}. This gives

$$(\gamma_{\boldsymbol{q}}^{DA})^2=a_{DA}\frac{\hbar^2 v_s q^2}{p_0^3\tau_{DA}}, \tag{13}$$

where $\hbar p_0=(2m^*\hbar\omega_0)^{1/2}$ and $a_{DA}=2\pi\alpha\xi^2/a$. ω_0 is the frequency of longitudinal-optical phonons, and m^* is the effective mass of the electrons.

C. Piezoelectric interaction

Along with the deformation potential interaction, the piezoelectric electron-phonon interaction appears in crystals

which lack a center of symmetry, cf., for example, Ref. 22. In this case, an elastic wave leads to a polarization $\boldsymbol{P}$ of the lattice,

$$P_j=\sum_{k,l}\tilde{\beta}_{jkl}u_{kl}, \tag{14}$$

where $\tilde{\beta}_{jkl}$ is the tensor of the piezoelectric moduli. The corresponding interaction Hamiltonian follows from the electric potential $\varphi(\boldsymbol{r},t)$ associated with the polarization, and reads

$$H_{PA}=e\varphi(\boldsymbol{r},t). \tag{15}$$

The polarization and the electric potential are related to one another via Poisson's equation

$$\mathrm{div}\boldsymbol{D}=\varepsilon_0\mathrm{div}(4\pi\boldsymbol{P}-\mathrm{grad}\varphi)=0, \tag{16}$$

where $\boldsymbol{D}$ is the dielectric displacement, and $\varepsilon_0\approx 12.8$ is the dielectric constant of GaAs.

In the case of interest here, the general expression (14) is simplified because the GaAs samples used in experiments are cubic crystals and a crystal cut is chosen [the (100) surface] where the surface is spanned by two lattice axes.[5] Then the tensor $\tilde{\beta}_{jkl}$ has only components in which all three indices j, k, and l differ from each other and all components are equal to $\beta/8\pi$. Hence Eq. (14) reduces to

$$P_x=(4\pi)^{-1}\beta u_{yz},\quad P_y=(4\pi)^{-1}\beta u_{zx},$$
$$P_z=(4\pi)^{-1}\beta u_{xy}. \tag{17}$$

Substituting the displacement field (9) into Eq. (7) for the strain tensor yields the polarization (17). Then the Poisson equation (16) for φ can be solved most easily by a Fourier transform in the x-y plane, leading to

$$\left[\frac{\partial^2}{\partial z^2}-q^2\right]\varphi(z,t)=\beta C q_x q_y e^{-i\omega_q t}[-3\kappa_l e^{-\kappa_l qz}$$
$$+f(1+2\kappa_t^2)e^{-\kappa_t qz}]+\mathrm{c.c.} \tag{18}$$

The solution of this inhomogeneous differential equation can be constructed in the usual way. Discarding the exponentially increasing term e^{qz}, one obtains that every mode with a wave vector $\boldsymbol{q}$ is associated with an electric potential

$$\varphi_{\boldsymbol{q}}(\boldsymbol{r},t)=\beta\xi^{-2}C\hat{q}_x\hat{q}_y e^{i(\boldsymbol{q}\cdot\boldsymbol{R}-\omega_q t)}\{3\kappa_l\alpha^{-1}e^{-\kappa_l qz}$$
$$-f(1+2\kappa_t^2)e^{-\kappa_t qz}+c_1 e^{-qz}\}+\mathrm{c.c.}, \tag{19}$$

where $\hat{q}_x=\boldsymbol{q}\cdot\hat{\boldsymbol{x}}/q$ and $\hat{q}_y=\boldsymbol{q}\cdot\hat{\boldsymbol{y}}/q$. We note that for the geometry under consideration the total number of decay lengths for the elastic displacements and the electric potential is three, cf. Ref. 2 for comments on the general case. c_1 is a constant of integration which is determined by the boundary conditions at the surface $z=0$. In view of the experiments, we assume that the surface of the crystal is an electrically free boundary[1] to vacuum. That is, the normal component of the dielectric displacement, Eq. (16), and the parallel components of the electric field are continuous at the surface,

$$4\pi\varepsilon_0 P_z-\varepsilon_0\frac{\partial}{\partial z}\varphi\Big|_{z=+0}=-\frac{\partial}{\partial z}\varphi\Big|_{z=-0}, \tag{20a}$$

$$\frac{\partial}{\partial\boldsymbol{R}}\varphi\Big|_{z=+0}=\frac{\partial}{\partial\boldsymbol{R}}\varphi\Big|_{z=-0}. \tag{20b}$$

Note that the boundary conditions (20) differ from the requirement $\varphi_{z=0}=0$ for a sample which is covered with a thin metallic film. An appropriate ansatz for the electric potential outside of the crystal ($z<0$) is $\varphi=c_2 e^{i(\boldsymbol{q}\cdot\boldsymbol{R}-\omega_q t)}e^{qz}$. Substituting this ansatz and the general solution (19) for $z>0$ into the boundary conditions (20) yields that the constant of integration is

$$c_1=\frac{1}{2\bar{\varepsilon}}[-3\kappa_l\alpha^{-1}(1+\kappa_l\varepsilon_0)+f(1+2\kappa_t^2)(1+\kappa_t\varepsilon_0)$$
$$-\varepsilon_0\xi^2(1-f\kappa_t)], \tag{21}$$

where $\bar{\varepsilon}=(\varepsilon_0+1)/2$ is the average of the dielectric constants of GaAs and the space above the sample surface (vacuum), respectively. For large values of ε_0, $\varepsilon_0\gg 1$, this result coincides with the one which follows from the approximate boundary condition $(\partial/\partial z)\varphi|_{z=-0}=0$, cf. Eq. (20a). The electric potential (19) associated with a single displacement mode is now completely determined.

Assigning the amplitudes $b_{\boldsymbol{q}}$ and $b_{\boldsymbol{q}}^\dagger$ to the first and second terms in Eq. (19), respectively, summing over all wave vectors, and introducing the result into the Hamiltonian (15), the piezoelectric vertex [see Eq. (11)] becomes

$$\gamma_{\boldsymbol{q}}^{PA}=\left(\frac{\hbar}{\rho v_s a}\right)^{1/2}\beta e\xi^{-2}\frac{\varepsilon_0}{2\bar{\varepsilon}}\hat{q}_x\hat{q}_y$$
$$\times[3\kappa_l\alpha^{-1}(1-\kappa_l)-f(1+2\kappa_t^2)(1-\kappa_t)$$
$$-\xi^2(1-f\kappa_t)], \tag{22}$$

where we set $z=0$ in $\varphi_{\boldsymbol{q}}(\boldsymbol{r},t)$, Eq. (19). Obviously, the strongest piezoelectric interaction occurs when the SAW is propagated along a diagonal direction ($\hat{q}_x\hat{q}_y=\pm\frac{1}{2}$). In the experiments just this piezoelectric active direction [$\boldsymbol{q}\|[011]$] is chosen. In terms of a nominal time τ_{PA} [cf. Eq. (13)], the interaction vertex reads

$$(\gamma_{\boldsymbol{q}}^{PA})^2=a_{PA}(\hat{q}_x\hat{q}_y)^2\frac{\hbar^2 v_s}{p_0\tau_{PA}}, \tag{23}$$

where all the numerical quantities are absorbed in the prefactor a_{PA}.

D. Discussion of the interaction vertices

Let us compare the results for the interaction vertices $\gamma_{\boldsymbol{q}}$ in the Hamiltonian (11) with those valid for 3D bulk phonons (or a fictitious 2D phonon system). There are two significant differences. First, the interaction vertices for SAW's have a different dependence on the wave vector: $|\gamma_{\mathrm{SAW}}|^2$ exhibits an additional factor q compared to $|\gamma_{\mathrm{bulk}}|^2$. This applies to both the deformation potential and the piezoelectric interaction. Consequently, the use of the SAW interaction vertices in calculations of various physical quantities can give rise to results which deviate from those which are based on the assumption of two- or three-dimensional phonon systems. Second, for surface phonons, the deformation potential and the piezoelectric interaction are *in* phase. This is in contrast to the case of bulk phonons

where these vertices are *out* of phase, i.e., they contribute additively to $|\gamma_{\rm bulk}|^2=|\gamma^{DA}_{\rm bulk}+\gamma^{PA}_{\rm bulk}|^2=|\gamma^{DA}_{\rm bulk}|^2+|\gamma^{PA}_{\rm bulk}|^2$; see, for example, Ref. 22. The absolute value squared of $\gamma_{\boldsymbol{q}}$ is the relevant quantity which determines the total electron-phonon interaction. Clearly, the out-of-phase or the in-phase property is of importance only when the interaction vertices for the deformation potential and the piezoelectric interaction are of the same order of magnitude. This depends on the wavelength of the SAW because γ^{PA}, Eq. (22), does not depend on the magnitude of q whereas γ^{DA}, Eq. (12), increases linearly with q. In the case of GaAs, the relative strength of these two interaction mechanisms is thus $\gamma^{DA}/\gamma^{PA}\approx q10^{-7}$cm, where we have used the numerical values given below. Thus for the range of wavelengths used in recent experiments on the attenuation of a SAW in GaAs samples (see, for example, Refs. 3–6, 8, and 23), the deformation-potential scattering can be neglected in comparison with the piezoelectric interaction, except for propagation along $\langle 100\rangle$ directions. This result corroborates very well with the fact that the experimental findings could be explained in terms of the piezoelectric electron-phonon coupling alone.[5]

For easy reference, we summarize the numerical values for the parameters appearing in the interaction vertices $\gamma_{\boldsymbol{q}}$. For GaAs, $c_l\approx 5\times 10^5$ cm/s, $c_t\approx 3\times 10^5$ cm/s, and, hence, $\alpha=0.36$. The corresponding solution of the algebraic equation[20] for ξ is $\xi\approx 0.9$. Substituting these values in Eq. (8) yields $a=1.4$. Using $\tau_{DA}=4$ ps, $\tau_{PA}=8$ ps, $\hbar\omega_0=421$ K (this corresponds to $\Xi=7.4$ eV and $e\beta=2.4\times 10^7$ eV/cm), and $\rho=5.3$ g/cm^3 (see Ref. 22), we obtain $\gamma^{DA}_{\boldsymbol{q}}=5.6\times 10^{-17}q$ eV cm^2 and $\gamma^{PA}_{\boldsymbol{q}}=3.7\hat{q}_x\hat{q}_y 10^{-10}$ eV cm.

The above calculations are restricted, with respect to the piezoelectric interaction, to cubic crystals and a particular crystal cut. It is straightforward, however, to perform calculations for different crystals or surfaces along the same lines.

III. ELECTRON STATES AND PERCOLATION THEORY

Consider a 2DEG in a strong magnetic field B perpendicular to the plane of the 2DEG and in a smooth potential $V(\boldsymbol{R})$ (see, for instance, the paper by Trugman[24] and references therein). The potential $V(\boldsymbol{R})$ is assumed to vary slowly on the scale of the magnetic length $l_B=\sqrt{c\hbar/eB}$. Electron-electron interactions are neglected. The wave function $\Psi(\boldsymbol{R})$ of a state with energy ϵ is appreciable only in the vicinity of an equipotential line (EL) of the potential $V(\boldsymbol{R})=\epsilon$. The width of the wave functions perpendicular to the EL is l_B. Explicitly, the electron states of the nth Landau level (LL) can be approximated, in the limit $B\to\infty$, by

$$\Psi(\boldsymbol{R})\equiv\Psi(u,v)=[\mathcal{T}v_D(u,v)]^{-1/2}\chi_n(v)e^{i\varphi(u,v)}. \quad (24)$$

[We have omitted the part $\Psi(z)$ of the wave function which corresponds to the lowest occupied subband perpendicular to the plane of the 2DEG.] The orthogonal variables u and v parametrize the distances along and perpendicular to the EL, respectively. The function $\chi_n(v)$ is the nth harmonic-oscillator function. Below, we shall restrict ourselves to the lowest Landau level, i.e., $n=0$. In Eq. (24), $\varphi(u,v)$ is a gauge-dependent phase, and $\mathcal{T}$ is the period associated with one revolution around the EL of an electron moving with the drift velocity v_D. That is,

$$\mathcal{T}=\oint du\,\frac{1}{v_D(u,v)}, \quad v_D=|\nabla V|l_B^2/\hbar. \quad (25)$$

For the wave function (24) to be single valued, $\varphi(u,v)$ has to change by an integral multiple of 2π around an EL. This condition leads to the quantization of the allowed constant-energy lines. In other words, only a discrete sequence of EL's corresponds to the electron eigenstates. Two adjacent eigenstates enclose an area $2\pi l_B^2$ and are, on the average, a distance $\Delta v\simeq l_B^2/\mathcal{L}$ apart, where $\mathcal{L}$ is the length of one of the EL's. An important quantity is the difference $\hbar\omega_{\mathcal{T}}$ of the corresponding eigenenergies, where the frequency $\omega_{\mathcal{T}}$ is determined by

$$\omega_{\mathcal{T}}=2\pi/\mathcal{T}. \quad (26)$$

The quasiclassical description of the electron states that we have outlined above is a valid approximation when[24]

$$l_B/r_c\ll 1 \quad \text{and} \quad m^*|\nabla V(\boldsymbol{R})|l_B^3/\hbar^2\ll 1, \quad (27)$$

where r_c is the local radius of curvature of the EL, and m^* is the effective electron mass. The first condition is related to the smoothness of the potential, while the second one prevents the mixing of different LL's. Additionally, one should keep in mind that quantum tunneling[25] between classical EL's is important when $|\epsilon|$ is smaller than $\Delta(l_B/\Lambda)^2$.

In what follows $V(\boldsymbol{R})$ is a smooth *random* potential. The potential is assumed to be Gaussian, with

$$\langle V(\boldsymbol{R})V(0)\rangle=\Delta^2\phi(R/\Lambda), \quad (28)$$

where $\Delta=\sqrt{\langle V^2\rangle}$ defines its amplitude and Λ its correlation length. (Δ determines also the broadening of the LL.) The zero of energy is chosen such that $\langle V(\boldsymbol{R})\rangle=0$, i.e., the energy ϵ is measured from the center of the lowest LL. Using Δ and Λ, we can rewrite the conditions (27) in the form

$$l_B/\Lambda\ll 1 \quad \text{and} \quad \frac{\Delta}{\hbar\omega_c}\frac{l_B}{\Lambda}\ll 1, \quad (29)$$

where $\omega_c=eB/cm^*$ is the cyclotron frequency. These conditions are fulfilled, for example, for the following experimental values: $B=10$ T ($l_B=8$ nm, $\omega_c=2\pi\times 4.2$ THz), $\Delta=1$ meV and $\Lambda=50$ nm. The separation between two consecutive LL's is much larger than their broadening, $\hbar\omega_c/\Delta\approx 60$.

As discussed in Ref. 18, most EL's with ϵ in the tail of the LL, i.e., $|\epsilon|\gg\Delta$, have diameters $\mathcal{D}$ which are small compared to Λ and their length $\mathcal{L}$ is of the order of $\mathcal{D}$. When the energy approaches the center of the LL, the size of the EL's grows.[26] In particular, for $|\epsilon|\simeq\Delta$, $\mathcal{L}\simeq\mathcal{D}\simeq\Lambda$ holds for most of the EL's. Such EL's will be denoted as standard. A further reduction of $|\epsilon|$ does not lead to an increase in the size of almost all EL's, i.e., most of them remain standard ones. However, a minority of the EL's merges and forms large extended EL's with diameters $\mathcal{D}\gg\Lambda$. The structure of these extended EL's is described by percolation theory[27] when the energies $|\epsilon|$ are near the percolation threshold $\epsilon=0$ (or

$|\epsilon|/\Delta \ll 1$). The subsequent calculations show that just this range of energies is of interest justifying the use of the percolation picture.

An extended EL has a fractal structure which is reflected in the relation between its length and diameter[27]

$$\mathcal{L} \simeq \Lambda (\mathcal{D}/\Lambda)^{2/\alpha}, \tag{30}$$

where $\alpha = 8/7$ is the scaling exponent. (For the definition of the perimeter of discrete percolation clusters and the transition to continuum percolation see, e.g., Refs. 28 and 26.) An extended EL can be viewed as a self-avoiding random walk path with steps of length Λ. Indeed, $2/\alpha = 7/4$ is close to the value 2 which applies to a simple random walk. The exponent is less than 2 due to the self-avoiding nature of the EL.

The distribution of extended EL's of a given energy ϵ is described by one scale, the so-called critical diameter

$$\mathcal{D}_c(\epsilon) \simeq \Lambda (|\epsilon|/\Delta)^{-\nu}, \tag{31}$$

which is considered to be the localization length in the semiclassical theory. The scaling index is $\nu = 4/3$. EL's with diameters $\mathcal{D} \gg \mathcal{D}_c(\epsilon)$ are exponentially rare, while the probability to find an extended EL with a diameter $\Lambda \ll \mathcal{D} \ll \mathcal{D}_c(\epsilon)$ is proportional to $\mathcal{D}^{-\rho}$, where $\rho = 3$.

An electron that moves on an extended EL ($\mathcal{L} \gg \Lambda$) experiences different regions of the random potential. During one revolution, the drift velocity $v_D(u,v)$ [see Eq. (25)] follows the varying slope of the potential $V(\boldsymbol{R})$ and takes on many different values. In other words, the motion on an extended EL corresponds to an averaging process with respect to $v_D(u,v)$. It is therefore reasonable to introduce an average drift velocity[18] $\overline{v_D}$, defined by $\mathcal{T} = \mathcal{L}/\overline{v_D}$, that is assumed to be independent of the length of the EL under consideration. The dependence on the energy ϵ can be generally excluded since $V(\boldsymbol{R})$ and $\nabla V(\boldsymbol{R}) \sim v_D(\boldsymbol{R})$ are statistically independent for a Gaussian distribution.[29] Consequently, the energy-level spacing (26) associated with the extended EL's is a function of $\mathcal{L}$ alone and Eq. (26) can be written conveniently in the form

$$\hbar \omega_{\mathcal{T}}(\mathcal{L}) = \hbar \Omega \frac{\Lambda}{\mathcal{L}}, \tag{32}$$

where

$$\hbar \Omega = \hbar \frac{2\pi \overline{v_D}}{\Lambda} \simeq \frac{\Delta l_B^2}{\Lambda^2}. \tag{33}$$

The frequency Ω gives by order of magnitude the level spacing for standard EL's since it is associated with the revolution around an EL with $\mathcal{L} \simeq \Lambda$. The corresponding frequencies for the extended EL's are lower. The lowest frequencies belong to the longest EL's which have the critical length $\mathcal{L}_c$ corresponding to the critical diameter $\mathcal{D}_c$ (31). From Eqs. (30) and (31),

$$\mathcal{L}_c(\epsilon) \simeq \Lambda |\Delta/\epsilon|^{2\nu/\alpha}. \tag{34}$$

Below, we shall use the distribution of the EL's with respect to their lengths. Let $L^2 f_\epsilon(\mathcal{L}) d\mathcal{L}$ be the number of EL's with energy ϵ and a length between $\mathcal{L}$ and $\mathcal{L} + d\mathcal{L}$. The normalization of this distribution can be found by equating the total average length of the EL's in an area of size L^2 to the result given in the literature (see Sec. III A in Refs. 29 or 30)

$$L^2 \int_0^\infty d\mathcal{L}\, \mathcal{L} f_\epsilon(\mathcal{L}) = \frac{L^2}{2\Lambda} [-\phi''(0)]^{1/2} \exp\left[-\frac{\epsilon^2}{2\Delta^2}\right], \tag{35}$$

where ϕ is defined in Eq. (28).

While the distribution of the standard EL's is not really known, percolation theory gives the following ansatz[27] for the distribution of extended EL's:

$$f_\epsilon(\mathcal{L}) d\mathcal{L} = C_\epsilon \left(\frac{\mathcal{L}}{\Lambda}\right)^{-[(\alpha/2)(\rho-1)+1]} G\left(\frac{\mathcal{L}}{\mathcal{L}_c(\epsilon)}\right) d\mathcal{L}, \quad \mathcal{L} \gg \Lambda, \tag{36}$$

where C_ϵ is the normalization constant and $G(\zeta)$ is a function which is exponentially small for $\zeta \gg 1$ and of order unity for $\zeta \ll 1$. Hence G yields a smooth cutoff of the distribution for $\mathcal{L} > \mathcal{L}_c$, where $\mathcal{L}_c$ is defined in Eq. (34). An additional, energy-independent cutoff appears in a finite sample. Here, the size L of the system restricts the critical diameter $\mathcal{D}_c$ (31) to values such that $\mathcal{D}_c \lesssim L$. This translates into $\mathcal{L} \lesssim \Lambda (L/\Lambda)^{2/\alpha}$, using Eq. (30). Thus, in a finite system, the critical length $\mathcal{L}_c(\epsilon)$ in Eq. (36) should be replaced by $\min\{\mathcal{L}_c(\epsilon), \Lambda (L/\Lambda)^{2/\alpha}\}$.

To find the normalization constant C_ϵ, let us decompose the normalization integral (35) into $\int_0^\Lambda + \int_\Lambda^\infty$ and estimate both terms of this decomposition. The second integral can be estimated from the distribution (36) of extended EL's. With the value $(\alpha/2)(\rho-1)+1 = \frac{15}{7}$, this integral is determined by its lower limit Λ and is of the order $(L\Lambda)^2$. Using a reasonable ansatz for the distribution of standard and short EL's (for example $f_\epsilon(\mathcal{L}) = \text{const}$), the first integral is determined by its upper limit Λ and is again of the order $(L\Lambda)^2$. Thus the total normalization integral is also of this order. Up to a factor of order unity, the normalization constant C_ϵ is then given by Λ^{-3}. The numerical factor can be absorbed in G leading to the following distribution function for extended EL's:

$$f_\epsilon(\mathcal{L}) d\mathcal{L} = \frac{1}{\Lambda^3} \left(\frac{\mathcal{L}}{\Lambda}\right)^{-[(\alpha/2)(\rho-1)+1]} G\left(\frac{\mathcal{L}}{\mathcal{L}_c(\epsilon)}\right) d\mathcal{L}. \tag{37}$$

We note that the above estimates confirm that the majority of EL's belongs to the standard ones with $\mathcal{L} \simeq \Lambda$, since these EL's are relevant in the normalization integral.

IV. MATRIX ELEMENTS

Emission and absorption of phonons are associated with electronic transitions with energy transfer $\hbar \omega_q$. We saw in Sec. III that the separation in energy between two consecutive EL's is given by $\hbar \omega_{\mathcal{T}}$ [Eq. (26)]. Thus *real* transitions are generally restricted to EL's for which $\omega_{\mathcal{T}} \lesssim \omega_q$. For the parameters used above for conditions (29), the frequency Ω, Eq. (33), is about $2\pi \times 10$ GHz, whereas the frequencies of the SAW's used in experiments vary typically in the range $\omega_q = 2\pi \times 1$ MHz/1 GHz. We therefore conclude that only extended EL's for which $\omega_{\mathcal{T}} = \Omega \Lambda/\mathcal{L} \ll \Omega$ [see Eq. (32)] contribute to the sound absorption. Thus the matrix elements of the interaction Hamiltonian (11)

$$\mathcal{M}_{if}^{\pm\mathbf{q}}=\frac{1}{L}\gamma_{\mathbf{q}}M_{if}^{\pm\mathbf{q}}\equiv\frac{1}{L}\gamma_{\mathbf{q}}\langle f|e^{\pm i\mathbf{q}\cdot\mathbf{R}}|i\rangle, \tag{38}$$

where $|i\rangle$ and $|f\rangle$ denote the initial and final wave functions of the form (24), have to be calculated for extended trajectories. This calculation has been performed in Ref. 18. The matrix element, averaged over all trajectories with the same period $\mathcal{T}$ and the same energy ϵ, reads

$$\langle|M_{if}^{\pm\mathbf{q}}|^2\rangle_{\epsilon,\mathcal{T}}=cq^2\Lambda^2(\hbar\Omega)^{\alpha}\frac{\hbar\omega_{\mathcal{T}}}{|\epsilon_f-\epsilon_i|^{\alpha+1}}$$
$$\text{for } |\epsilon_f-\epsilon_i|\lesssim\hbar\Omega, \tag{39}$$

where c is a numerical factor of order unity. The matrix element is valid under the assumptions $q\Lambda\ll v_D/v_s\ll(q\Lambda)^{-3/4}$, where the exponent $\frac{3}{4}$ follows from $(2-\alpha)/\alpha$ with $\alpha=\frac{8}{7}$, cf. Eq. (30). Clearly, these inequalities imply $q\Lambda\ll1$.

For $|\epsilon_f-\epsilon_i|\gg\hbar\Omega$, the matrix element $\langle|M_{if}^{\pm\mathbf{q}}|^2\rangle_{\epsilon,\mathcal{T}}$ is exponentially small. This implies that transitions occur only within the lowest LL, and that transitions to other LL's can be neglected ($\hbar\omega_c\gg\Delta\gg\hbar\Omega$). It is also assumed that the initial and final states are close to one another in real space: In order that $(\chi_0)_i$ and $(\chi_0)_f$ will overlap, the separation in real space, Δv, should satisfy $\Delta v\lesssim l_B$. The condition $|\epsilon_f-\epsilon_i|\lesssim\hbar\Omega$ is even more restrictive. This can be seen in the following way. As mentioned above, the mean distance in real space between two adjacent EL's is given by $l_B^2/\mathcal{L}$. Hence, the distance between the two states i and f is of order $(l_B^2/\mathcal{L})|\epsilon_f-\epsilon_i|/\hbar\omega_{\mathcal{T}}$. The maximum of this expression is found for the largest allowed energy difference $|\epsilon_f-\epsilon_i|\simeq\hbar\Omega$. Using the definition of $\omega_{\mathcal{T}}$ in Eq. (32) and the estimate for Ω in Eq. (33), the corresponding maximum distance in real space is found to be $l_B^2/\Lambda\ll l_B$, cf. inequalities (29).

While the sound absorption is due to transitions between extended states, the calculation of the dielectric function (see Sec. V) also necessitates matrix elements between standard EL's. (Transitions between a standard EL and an extended EL are exponentially rare due to their large separation in space.) Since the majority of the EL's belongs to the standard ones, one might even expect that the standard EL's dominate the dielectric function. This is not the case, as is shown below.

Noting that for typical phonon wave vectors (e.g., $q\approx10^4\ \mathrm{cm}^{-1}$), one has $q\Lambda\ll1$, the matrix element for standard EL's with $\mathcal{L}\simeq\Lambda$ can be approximated by

$$\langle f|e^{i\mathbf{q}\cdot\mathbf{R}}|i\rangle=e^{i\mathbf{q}\cdot\mathbf{R}_i}\langle f|e^{i\mathbf{q}(\mathbf{R}-\mathbf{R}_i)}|i\rangle\approx e^{i\mathbf{q}\cdot\mathbf{R}_i}i\mathbf{q}\langle f|\mathbf{R}-\mathbf{R}_i|i\rangle, \tag{40}$$

where the zero-order term in the expansion of the exponential function disappears due to the orthogonality of the two states i and f. The vector $\mathbf{R}_i$ denotes some point in the vicinity of the ith EL. The matrix element on the right-hand side of Eq. (40) is of order Λ. Hence, for transitions between two standard EL's,

$$\langle|M_{if}^{\pm\mathbf{q}}|^2\rangle_{\epsilon,\mathcal{T}}\approx q^2\Lambda^2, \tag{41}$$

where it is understood that the EL's i and f are very close in real space and in energy; otherwise the matrix element is exponentially small. The first condition guarantees the overlap of the wave functions $\chi_0^{i(f)}$; see Eq. (24). The second one is necessary to ensure that the integrand of the u integration along the perimeter of the EL's is not a quickly oscillating function. Result (41) agrees essentially with Eq. (39) replacing there the energy difference $|\epsilon_f-\epsilon_i|$ and the level spacing $\hbar\omega_{\mathcal{T}}$ by the value $\hbar\Omega$ appropriate for standard EL's.

V. DIELECTRIC FUNCTION

The matrix element (38) includes the screening of the electron-phonon interaction due to the lattice [Eq. (22)]. The screening arising from the 2DEG can be accounted for by renormalizing the matrix element

$$|\mathcal{M}_{if}^{\pm\mathbf{q}}|^2\to\frac{|\mathcal{M}_{if}^{\pm\mathbf{q}}|^2}{|\varepsilon(\omega_q,q)|^2}, \tag{42}$$

where $\varepsilon(\omega,q)$ is the dielectric function of the 2DEG. For a nearly half-filled LL, the dielectric function can be calculated assuming linear screening.[31] That is, the change in the electron density resulting from a small applied potential is proportional to the strength of the perturbing potential. Indeed, one can estimate that for the SAW intensities used in experiments the electron density oscillates only weakly around its average value; see, for example, Ref. 7. The assumption of linear screening leads to the general expression

$$\varepsilon(\omega,q)=1+\frac{2\pi e^2}{\overline{\varepsilon}q}\Pi(\omega,q), \tag{43}$$

where

$$\Pi(\omega,q)=\frac{1}{L^2}\sum_{i\neq f}\frac{f(\epsilon_i)-f(\epsilon_f)}{\epsilon_f-\epsilon_i-\hbar\omega-i0}|M_{if}^{\mathbf{q}}|^2, \tag{44}$$

and $\overline{\varepsilon}$ is defined in Eq. (21).

To evaluate Π explicitly, we transform the sum $\Sigma_{i\neq f}$ in Eq. (44) into $\Sigma_{i<f}$, where $i<f$ means $\epsilon_i<\epsilon_f$. Let us first focus on the case of zero temperature, i.e., all levels below the Fermi energy ϵ_F are occupied, $f(\epsilon_i)=1$, whereas all levels above ϵ_F are empty, $f(\epsilon_f)=0$. Then

$$\Pi(\omega,q)=\frac{2}{L^2}\sum_{i<f}\frac{\epsilon_f-\epsilon_i}{(\epsilon_f-\epsilon_i)^2-(\hbar\omega+i0)^2}|M_{if}^{\mathbf{q}}|^2. \tag{45}$$

In order to yield an appreciable matrix element, EL's corresponding to ϵ_i and ϵ_f must be close (in real space and in energy) to an EL with $\epsilon=\epsilon_F$. This Fermi EL (FEL) need not to be an electron state. We can therefore represent the summation over states in Eq. (45) as a sum over EL's near a certain FEL and then sum over all FEL's. In the first sum the states are distributed nearly equidistantly with an energy spacing $\hbar\omega_{\mathcal{T}}\approx$ const, cf. below. In the summation over FEL's we may first sum over the FEL's with the same period $\mathcal{T}$. Since these EL's are situated in different regions of the random potential, this summation is equivalent to an average of the matrix element over FEL's with the same period. Thus the averaged matrix elements (39) and (41) for extended and standard EL's, respectively, can be substituted in Eq. (45).

We begin with the contribution of the extended EL's to Π. As we shall see, this is the dominant contribution. It is

easy to see that the energy spacing for the relevant states near a fixed FEL is given by the value of $\hbar\omega_{\mathcal{T}}$ at the Fermi energy. To this end, we have to calculate the change in $\omega_{\mathcal{T}}$ arising from a change in the energy of the EL by at most $\hbar\Omega$ [see Eq. (39)]. Since the frequency $\omega_{\mathcal{T}}$ for the extended EL's is merely a function of $\mathcal{L}$, one has $\Delta\omega_{\mathcal{T}}/\omega_{\mathcal{T}} \simeq \Delta\mathcal{L}/\mathcal{L} \simeq \Delta\mathcal{A}/\mathcal{A}$, where $\mathcal{A}$ is the area enclosed by the EL. To obtain the second equality, we have used $\mathcal{L} \simeq \Lambda(\mathcal{A}/\Lambda^2)^{\lambda}$, with[27] $\lambda = \frac{12}{13}$. The change in the enclosed area is given by $2\pi l_B^2 \Omega/\omega_{\mathcal{T}}$, and thus $\Delta\omega_{\mathcal{T}}/\omega_{\mathcal{T}} \simeq (l_B^2/\Lambda^2)(\Lambda/\mathcal{L})^{1/\lambda - 1} \ll 1$. Consequently, the sum over EL's which are near a given FEL can be simplified by introducing an explicit representation for the energies

$$\epsilon_f - \epsilon_i = (m-n)\hbar\omega_{\mathcal{T}}. \tag{46}$$

The integers m and n are subject to the restrictions $|m-n| \lesssim \Omega/\omega_{\mathcal{T}}$ [see Eq. (39)] and $m-n \neq 0$. Using representation (46) and matrix element (39), the double sum over states near one FEL in Eq. (45) can be reduced to a sum over $s = m-n$, and one obtains

$$\sum_{i<f} \frac{1}{(\epsilon_f - \epsilon_i)^2 - (\hbar\omega + i0)^2} \frac{\hbar\omega_{\mathcal{T}}}{|\epsilon_f - \epsilon_i|^{\alpha}} = \left(\frac{x}{\hbar\omega}\right)^{\alpha+1} S(x), \tag{47}$$

where $x = \omega/\omega_{\mathcal{T}}$ and

$$S(x) \equiv \sum_{s=1}^{\infty} \frac{1}{s^2 - (x+i0)^2} \frac{1}{s^{\alpha-1}}. \tag{48}$$

We have replaced the upper limit in the sum by infinity, since the relevant s are of order $x \ll \Omega/\omega_{\mathcal{T}}$, and the above-mentioned restriction for $|m-n|$ can be neglected. In other words, the EL's which contribute significantly are separated in energy by $\hbar\omega$.

For extended states, using Eq. (32), $x = (\omega/\Omega)(\mathcal{L}/\Lambda)$, and hence the contribution to $\Pi(\omega,q)$ from a FEL is a function of its length alone. As a result the total $\Pi(\omega,q)$ can be written as a sum over all lengths. Using the distribution function $f_{\epsilon}(\mathcal{L})$ given in Eq. (37), we find

$$\begin{aligned}\Pi(\omega,q;\epsilon_F) &= 2c\frac{(q\Lambda)^2\Omega^{\alpha}}{\hbar\omega^{\alpha+1}} \int d\mathcal{L} f_{\epsilon_F}(\mathcal{L}) x^{\alpha+1} S(x) \\ &= 2c\frac{q^2}{\hbar\omega} H(y_F),\end{aligned} \tag{49}$$

where

$$y_F = \frac{\Omega\Lambda}{\omega\mathcal{L}_c(\epsilon_F)} = \left|\frac{\epsilon_F}{\epsilon_{\omega}}\right|^{2\nu/\alpha} \quad \text{and} \quad \epsilon_{\omega} = \Delta\left(\frac{\omega}{\Omega}\right)^{\alpha/2\nu}. \tag{50}$$

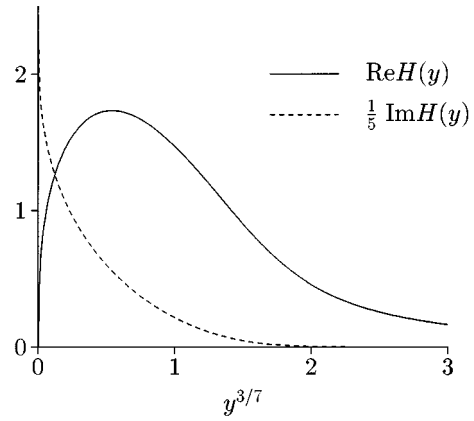

FIG. 1. The real and imaginary parts of the function $H(y)$ defined in Eqs. (52). $G(z)$ was replaced by $2/[\exp(z)+1]$. The particular choice of the function G has no influence on the qualitative behavior of H when the cutoff introduced by G is smooth enough to wash out all discrete features of the sums in Eqs. (52). The following figures are based on the curves of H given here.

In a finite system of size L, y_F has to be replaced by the maximum of y_F and $y_L \equiv (\Omega/\omega)(\Lambda/L)^{2/\alpha}$, see the discussion following Eq. (36). Using the explicit form for the distribution function f with $\rho = 3$ yields

$$H(y) = \int_0^{\infty} dx\ G(xy) S(x). \tag{51}$$

The quantity ϵ_{ω} has a very intuitive interpretation: it is the energy at which the energy level spacing $\hbar\omega_{\mathcal{T}}(\mathcal{L}_c(\epsilon))$ for an EL with the critical length is equal to the phonon energy $\hbar\omega$ of the SAW. In other words, ϵ_{ω} determines the absorption threshold in the sense that real transitions occur only for $|\epsilon_F| \lesssim \epsilon_{\omega}$. This is reflected in the imaginary part of Π, calculated below.

The real and imaginary parts of the function H are given by

$$\mathrm{Re}H(y) = \int_0^{\infty} dx\ G(xy) \sum_{s=1}^{\infty} \frac{1}{s^{\alpha-1}} \frac{P}{s^2 - x^2}, \tag{52a}$$

$$\mathrm{Im}H(y) = \frac{\pi}{2} \sum_{s=1}^{\infty} \frac{1}{s^{\alpha}} G(sy), \tag{52b}$$

where P denotes the principal part of the integral. The behavior of $H(y)$ in an infinite system is shown in Fig. 1. The y axis in Fig. 1 has been scaled in terms of $y^{3/7}$ corresponding to the dependence of H on the Fermi energy; see Eq. (50). The limiting behaviors for large and small arguments are given by

$$\begin{aligned} &\mathrm{Re}H \approx \zeta(1+\alpha)/y = 1.5/y, \quad \mathrm{Im}H \approx (\pi/2)G(y), \quad y \gg 1, \\ &\mathrm{Re}H \simeq y^{\alpha-1}, \quad \mathrm{Im}H \simeq 1 - y^{\alpha-1}, \quad y \ll 1, \\ &\mathrm{Re}H = 0, \quad \mathrm{Im}H = (\pi/2)\zeta(\alpha) = 11.9, \quad y = 0, \end{aligned} \tag{53}$$

where $\zeta(x)=\Sigma_{s=1}^{\infty}s^{-x}$. In order to discuss the analytic expressions of $H(y)$ we note that the sum in Eq. (52b) and the integral in Eq. (52a) are truncated at s or x of order $1/y$, as implied by G, Eq. (36). The imaginary part (52b) is therefore exponentially small $\sim G(y)$ for $y\gg 1$, and of order unity in the opposite case. Thus, the sum over s increases with decreasing y, and approaches its maximum as y goes to zero. In a finite system, y is restricted from below by y_L imposing an upper limit $1/y_L$ on the sum. This leads to a smaller maximum value of ImH. As for the real part of $H(y)$, we are able to study the limiting cases. For both $y\gg 1$ and $y\ll 1$, Re$H(y)$ goes to zero according to a power law. In the intermediate region $y\lesssim 1$ but not $y\ll 1$, ReH is slowly varying and of order unity. In a finite system, the real part approaches a small but finite value as y goes to y_L.

Up to this point, the evaluation of Π, Eq. (44), has been performed for zero temperature, $T=0$. The calculation of Π for finite temperatures such that $T\gg\hbar\omega$ can be done along the same lines. Therefore, we give only a brief description. The calculations for $T=0$ have shown that the real and imaginary parts of H reach a value of order unity when the Fermi energy becomes of order ϵ_ω. This energy range corresponds to the contribution of EL's with a length $\mathcal{L}_\omega\equiv\mathcal{L}_c(\epsilon_\omega)\simeq\Lambda(\Omega/\omega)$, and an energy-level spacing of order $\hbar\omega$ to the transition processes. Therefore, these extended EL's make the dominant contributions to Π, Eq. (44). This remains true for finite temperatures. However, now states i and f need not be in the immediate vicinity of the FEL's. Instead, we can fix some initial state i and consider transitions to final states above, $\epsilon_f>\epsilon_i$, and below, $\epsilon_f<\epsilon_i$, the chosen one (essentially in a range T around ϵ_F). To do this, we use representation (46), where $\omega_{\mathcal{T}}$ now refers to the energy ϵ_i. Expanding the Fermi distribution $f(\epsilon_f)$ in Eq. (44) around ϵ_i leads to $-\partial f(\epsilon_i)/\partial\epsilon_i$ (for the relevant transitions, $|\epsilon_f-\epsilon_i|$ is much smaller than T). The sum over the energies ϵ_f is reduced to twice expression (48). Hence

$$\Pi(\omega,q)=2c\left(\frac{q\Lambda}{L}\right)^2(\hbar\Omega)^{\alpha}\sum_i\left(-\frac{\partial f}{\partial\epsilon_i}\right)(\hbar\omega_{\mathcal{T}})^{-\alpha}S\left(\frac{\omega+i0}{\omega_{\mathcal{T}}}\right). \tag{54}$$

The sum over the initial states i comprises a summation over all EL's with the same energy ϵ_i but with different lengths $\mathcal{L}$, and a summation over ϵ_i. The first sum can be again replaced by an integral using the distribution function $f_\epsilon(\mathcal{L})$, Eq. (37). Then the order of summation and integration is inverted to obtain

$$\sum_{\epsilon_i}\int_0^\infty d\mathcal{L}\rightarrow\int_0^\infty d\mathcal{L}\sum_{|\epsilon_i|\lesssim\epsilon_c(\mathcal{L})}\rightarrow\int_0^\infty d\mathcal{L}\int_{-\infty}^{\infty}\frac{d\epsilon_i}{\hbar\omega_{\mathcal{T}}(\mathcal{L})}. \tag{55}$$

The condition $|\epsilon_i|\lesssim\epsilon_c(\mathcal{L})$ ensures that only those initial states which possess a critical length $\mathcal{L}_c$ equal to or larger than $\mathcal{L}_c(\epsilon_i)$ are included. Here $\epsilon_c(\mathcal{L})\simeq\Delta(\Lambda/\mathcal{L})^{\alpha/2\nu}$; see Eq. (34). However, the dominant contributions to Σ_{ϵ_i} follow from a particular group of EL's, rendering this condition unnecessary. Taking also into account that the relevant EL's have an energy-level spacing which is small compared to the thermal energy $\hbar\omega/T\ll 1$, and that the number of states per energy interval is given by $(\hbar\omega_{\mathcal{T}})^{-1}$, the sum over ϵ_i can be replaced by the integral given on the right-hand side of Eq. (55). The limits of integration have been extended with negligible error. The resulting integral over $\mathcal{L}$ coincides with the right-hand side of Eq. (49) except for the value of the energy: instead of the fixed Fermi energy ϵ_F, there appears now the variable ϵ_i. Thus we finally arrive at

$$\Pi(\omega,q)=\int_{-\infty}^{\infty}d\epsilon\left(-\frac{\partial f}{\partial\epsilon}\right)\Pi(\omega,q;\epsilon), \tag{56}$$

where we have dropped the index i of ϵ_i. This equation shows that a finite temperature leads to an average of the $T=0$ result over energies within an interval of order T around the Fermi level. Since the function $\Pi(\omega,q;\epsilon)$ varies on the scale ϵ_ω, finite-temperature effects are negligible if $T\ll\epsilon_\omega$. This is the condition for Eq. (49) to hold. For $T\gtrsim\epsilon_\omega$, the width of $\Pi(\omega,q)$ as function of the Fermi energy increases with temperature, i.e., the behavior of Π deviates substantially from the $T=0$ result. In the following we assume $T<\epsilon_\omega$.

Substituting the $T=0$ result for $\Pi(\omega,q)$ [Eq. (49), which is based on transitions between extended EL's] in Eq. (43) yields, for the dielectric function,

$$\varepsilon(\omega,q)=1+\frac{2\pi e^2}{\overline{\varepsilon}}\frac{q}{\hbar\omega}2cH(y_F), \tag{57}$$

and, for the renormalization of the matrix element in Eq. (42),

$$\varepsilon(\omega_q,q)=1+\frac{e^2}{\overline{\varepsilon}\hbar v_s}4\pi cH(y_F). \tag{58}$$

The contribution to the dielectric function resulting from standard EL's is derived below; see Eq. (59). The comparison of that result with Eqs. (57) and (58) shows that the dielectric function is essentially given by the contribution due to extended EL's, whereas the influence of transitions between standard EL's can be neglected. We therefore consider Eq. (58) as the final result for $\varepsilon(\omega_q,q)$.

The dielectric function (58) renormalizes the matrix element (42) via the expression $|\varepsilon(\omega_q,q)|^2$. The dependence of $|\varepsilon|^2$ on the Fermi energy is given by $|H|^2$, Eqs. (52). The latter is of order unity for $|\epsilon_F|\lesssim\epsilon_\omega$ and decreases for larger values of the Fermi energy according to the power law $(\epsilon_\omega/|\epsilon_F|)^{4\nu/\alpha}$, $4\nu/\alpha=\frac{14}{3}$. Thus the magnitude of ε, Eq. (58), is determined by the large dimensionless parameter $e^2/\overline{\varepsilon}v_s\hbar$ (≈ 110 for GaAs). This is the ratio of the electrostatic energy of two electrons a distance q^{-1} apart and the energy of a surface phonon $(e^2q/\overline{\varepsilon})(\hbar\omega_q)^{-1}$.

Let us now show that the contribution of the standard EL's to the dielectric function is negligible. We start afresh from expression (45) for Π, substituting the matrix element (41) for transitions between standard EL's. The energy difference between two standard EL's is of order $\hbar\Omega$, Eq. (32), i.e., much larger than $\hbar\omega$. The latter can thus be neglected in comparison with $\epsilon_f-\epsilon_i$ in Eq. (45). Then the imaginary term $i0$ can be dropped, as no real transitions can occur. The sum over all final states f leads merely to a factor of order 1, since only a few EL's in the immediate vicinity of the initial EL contribute to the matrix element (41). The remaining sum

over the initial states counts the standard EL's which are just below the Fermi level. The number of these EL's is essentially the number of all FEL's, because the number of very short ($\mathcal{L}\ll\Lambda$) and very long ($\mathcal{L}\gg\Lambda$) EL's is negligibly small for Fermi energies near the center of the LL. The required quantity may therefore be deduced from Eq. (35), which states that the total length of all EL's is, up to a numerical factor, equal to $L^2/\Lambda=\Lambda(L^2/\Lambda^2)$. Since the mean length of all EL's is of order Λ, the number of FEL's in a system of size L is of order L^2/Λ^2.

Collecting these results, we obtain the contribution due to standard EL's,

$$\Pi(\omega,q)\simeq\frac{q^2}{\hbar\Omega}\quad\text{and}\quad\varepsilon(\omega,q)-1\simeq\frac{e^2q}{\overline{\varepsilon}\hbar\Omega}. \tag{59}$$

It can be shown that this estimate is valid independent of the ratio $\hbar\Omega/T$ as long as $\max\{\hbar\Omega,T\}\ll\Delta$. The comparison of Eqs. (59) and (57) shows that the contribution of the standard EL's to the dielectric function is ω/Ω times smaller than the term resulting from the extended EL's.

It is instructive to consider briefly an alternative derivation of the dielectric function which reproduces correctly the order of magnitude $|\varepsilon|\simeq e^2/\overline{\varepsilon v}_s\hbar$. This derivation relies on the fact that the motion of an electron on a fractal trajectory can be considered as a self-avoiding random walk with single steps of length Λ. In fact, the relation between the diameter and the length of an extended EL is similar to what one would expect for a simple random walk; cf. Eq. (30). For the diffusive regime, the density correlator Π, Eq. (44), is given by

$$\Pi(\omega,q)=g_F\frac{Dq^2}{-i\omega+Dq^2}, \tag{60}$$

where D is the diffusion constant and g_F the density of states at the Fermi level. In our case, we can assume $D\simeq v_D\Lambda$. The density of states of the LL is given by $g_F\simeq(\Delta l_B^2)^{-1}$ for $\epsilon_F\ll\Delta$. Substituting these quantities into Eq. (43) yields

$$\varepsilon(\omega_q,q)-1\simeq i\frac{e^2}{\overline{\varepsilon v}_s\hbar}, \tag{61}$$

where the term Dq^2 has been neglected compared to $-i\omega_q$ in the denominator of the density correlator. Interestingly, this approach predicts an essentially imaginary result for $\varepsilon-1$ which agrees with the behavior of Eq. (58) for $|\epsilon_F|\to0$, i.e., in the case when some the EL's become arbitrarily long.

VI. SURFACE ACOUSTIC-WAVE ATTENUATION

The intensity of the SAW decreases due to absorption of phonons by the 2DEG with the distance x as $\exp(-\Gamma x)$. The attenuation coefficient Γ can be expressed in terms of the sound velocity v_s [cf. Eq. (4)] and the life time $\tau(\boldsymbol{q})$ as $\Gamma=(v_s\tau(\boldsymbol{q}))^{-1}$, where $\tau(\boldsymbol{q})$ is defined by the rate equation

$$\dot{N}_{\boldsymbol{q}}=-\frac{1}{\tau(\boldsymbol{q})}N_{\boldsymbol{q}}. \tag{62}$$

Here $N_{\boldsymbol{q}}$ is the phonon occupation number. The net change in $N_{\boldsymbol{q}}$ is given by

$$\dot{N}_{\boldsymbol{q}}=\frac{2\pi}{\hbar|\varepsilon(\omega_q,q)|^2}\sum_{i\neq f}f(\epsilon_i)(1-f(\epsilon_f))[|\mathcal{M}_{if}^{-\boldsymbol{q}}|^2(N_{\boldsymbol{q}}+1)\times\delta(\epsilon_i-\epsilon_f-\hbar\omega_q)-|\mathcal{M}_{if}^{+\boldsymbol{q}}|^2N_{\boldsymbol{q}}\delta(\epsilon_i-\epsilon_f+\hbar\omega_q)], \tag{63}$$

where $f(\epsilon)$ is the Fermi distribution function and $\mathcal{M}_{if}^{\mp\boldsymbol{q}}$ are the unscreened matrix elements (38) for emission or absorption of a phonon with wave vector $\boldsymbol{q}$. For a SAW induced by interdigital transducers, the phonon occupation number $N_{\boldsymbol{q}}$ is macroscopically large. The difference between $N_{\boldsymbol{q}}+1$ and $N_{\boldsymbol{q}}$ is therefore negligible. Combining Eqs. (62) and (63) yields

$$\frac{1}{\tau(\boldsymbol{q})}=\frac{2\pi}{\hbar|\varepsilon(\omega_q,q)|^2}\sum_{i\neq f}|\mathcal{M}_{if}^{\boldsymbol{q}}|^2[f(\epsilon_i)-f(\epsilon_f)]\times\delta(\epsilon_i-\epsilon_f+\hbar\omega_q). \tag{64}$$

Replacing the δ function by the imaginary part of $-\pi^{-1}[\epsilon_i-\epsilon_f+\hbar\omega_q+i0]^{-1}$, we find

$$\frac{1}{\tau(\boldsymbol{q})}=\frac{2}{\hbar}\frac{|\gamma_{\boldsymbol{q}}|^2}{|\varepsilon(\omega_q,q)|^2}\mathrm{Im}\Pi(\omega_q,q)_{\omega_q>0}, \tag{65}$$

where Π is defined by Eq. (44).

Using the zero-temperature results for Π and the dielectric function, Eqs. (49) and (58), respectively, as well as the relation between the lifetime $\tau(\boldsymbol{q})$ and the attenuation coefficient, we find

$$\Gamma=\Gamma_q\Phi(y_F),\quad y_F=|\epsilon_F/\epsilon_\omega|^{2\nu/\alpha}, \tag{66}$$

with

$$\Gamma_q=\frac{1}{4\pi^2c\ \mathrm{Im}H(0)}|\gamma_{\boldsymbol{q}}|^2\frac{q\overline{\varepsilon^2}}{e^4}$$

and

$$\Phi(y)=\mathrm{Im}H(0)\frac{\mathrm{Im}H(y)}{|H(y)|^2}, \tag{67}$$

where the term 1 in expression (58) for ε has been neglected. The function $\Phi(y)$ is defined such that $\Phi(0)=1$ [since $\mathrm{Re}H(0)=0$, cf. Eqs. (53)], i.e., Γ_q coincides with the attenuation coefficient at the center of the LL, $\Gamma(\epsilon_F=0)=\Gamma_q$. We begin with the discussion of the magnitude of Γ_q and consider the function $\Phi(y)$ afterwards.

Substituting expressions (13) and (23) for the interaction vertices in Eqs. (67) yields

$$(\Gamma_q)_{DA}=\frac{a_{DA}}{4\pi^2c\ \mathrm{Im}H(0)}\frac{q^3}{v_sp_0^3\tau_{DA}}\left(\frac{\overline{\varepsilon v}_s\hbar}{e^2}\right)^2=2.6\times10^{-21}q^3\ \mathrm{cm}^2, \tag{68a}$$

$$(\Gamma_q)_{PA}=\frac{a_{PA}}{4\pi^2c\ \mathrm{Im}H(0)}\frac{q}{v_sp_0\tau_{PA}}\left(\frac{\overline{\varepsilon v}_s\hbar}{e^2}\right)^2=8.0\times10^{-6}q. \tag{68b}$$

That is, despite the fractal structure of the extended EL's on which these results are based, the frequency dependence of

the magnitude of Γ is simple and is not characterized by scaling exponents. Moreover, Γ_q is independent of the magnetic field and the parameters Λ and Δ of the random potential. The numerical values on the right-hand side of Eqs. (68) have been calculated replacing the parameters p_0, τ_{DA}, etc. by their values given in Sec. II, and assuming $c=1$. For a finite system, $\mathrm{Im}H(0)$ [see Eqs. (53)] has to be replaced by $\mathrm{Im}H(y_L)<\mathrm{Im}H(0)$; see the discussion following Eq. (50), leading to an increase of the attenuation coefficient at the center of the LL.

The function $\Phi(y_F)$ in Eq. (66) accounts for the dependence of Γ on the Fermi energy (or the filling factor ν or the magnetic field B). This dependence is determined by the ratio of $|\epsilon_F|$ and the energy $\epsilon_\omega=\Delta(\omega_q/\Omega)^{\alpha/2\nu}$ as follows. The absorption of the SAW is very small when the Fermi energy is far from the center of the LL $|\epsilon_F|\gg\epsilon_\omega$, i.e., $y_F\gg 1$. A strong increase of Φ and, hence, of Γ occurs when $|\epsilon_F|$ is reduced to $|\epsilon_F|\approx\epsilon_\omega$. In this region the number of occupied extended EL's with an energy-level spacing $\hbar\omega_{\mathcal{T}}(\mathcal{L})\lesssim\hbar\omega_q$, Eq. (32), undergoes the change from an exponentially small quantity to some power-law function of $\mathcal{L}^{-1}$. (Nevertheless, the number of these states is negligible compared to the majority of EL's with $\mathcal{L}\simeq\Lambda$.) A further rise of the absorption is prevented by the enhanced screening $\sim(\mathrm{Im}H)^2$ at $|\epsilon_F|\ll\epsilon_\omega$, which even reduces Γ as the Fermi energy goes to zero. This results in a shallow double-peak structure with a cusp at the center of the LL. In fact, if we use the limiting forms of $H(y\ll 1)$, Eqs. (53), we find $d\Gamma/d\epsilon_F\simeq\mathrm{sgn}(\epsilon_F)/|\epsilon_F|^{2\nu(2-\alpha)/\alpha}$. We believe, therefore, that the double-peak structure of $\Gamma(\epsilon_F)$ is independent of the function $G(z)$ used to describe the exponential cutoff of the extended EL's; see the discussion following Eq. (36). The maxima of $\Gamma(\epsilon_F)$ are located near $\pm\epsilon_\omega$; see Fig. 2. It is clear, however, that such a particular feature as the cusp has to be considered with caution, for it is exclusively based on the quasiclassical model for the electron states. Quantum tunneling between critical trajectories may modify this result. It is worth noting that the tunneling band of width[25] Ω [Eq. (33)] around $\epsilon=0$ [cf. the discussion after Eq. (27)] is narrow compared to the characteristic energy range ϵ_ω; indeed, $\Omega/\epsilon_\omega\approx(l_B/\Lambda)\sqrt{\omega/\Delta}\ll 1$. One may speculate that the absorption coefficient is only weakly affected by quantum tunneling. Indeed, most of the EL's contributing to Γ cannot be connected by low saddle points with transmission coefficients of order unity, and so quantum tunneling in-between them is insignificant.

To simplify the estimates, we rewrite ϵ_ω in the form

$$\epsilon_\omega=0.3\ \mathrm{meV}\left(\frac{\Delta}{1\ \mathrm{meV}}\right)^{4/7}\left(\frac{\omega_q}{2\pi\times 1\ \mathrm{GHz}}\right)^{3/7}\times\left(\frac{\Lambda}{50\ \mathrm{nm}}\right)^{6/7}\left(\frac{B}{5\ \mathrm{T}}\right)^{3/7}. \tag{69}$$

As discussed in Sec. V, the zero-temperature result (49) for Π remains valid for finite temperatures such that $T\ll\epsilon_\omega$. This is also the condition for Eq. (66) to hold. Using the values for Δ and Λ given above and $\omega_q=2\pi\times 100$ MHz, we obtain $\epsilon_\omega\approx 1$ K. For temperatures of the order of or larger than ϵ_ω, the attenuation coefficient is found from Eq. (65) using expression (56) in the calculation of the dielectric function and $\mathrm{Im}\Pi$. Two results for Γ at finite temperatures are shown in Fig. 2. With increasing temperature the minimum of the attenuation near the center of the LL is reduced and the absorption peak becomes broader. The increasing magnitude of Γ results from the significant broadening of the imaginary part of Π and the reduced screening; see Eq. (65). For $T\gtrsim\epsilon_\omega$, the magnitude of Γ and the width of the absorption region are strongly temperature dependent.

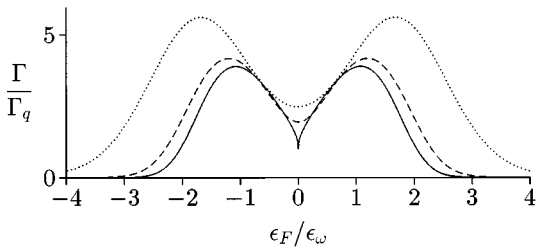

FIG. 2. The attenuation coefficient Γ, Eq. (66), as a function of the Fermi energy near the center of the lowest Landau level $\epsilon=0$. The three curves correspond to the following temperatures: $T=0$ (solid line), $T=0.15\epsilon_\omega$ (broken line), and $T=0.3\epsilon_\omega$ (dotted line).

The dependence of Γ on the SAW frequency ω_q is shown in Fig. 3. The curve is calculated for the low-temperature regime $T\ll\epsilon_\omega$ and the piezoelectric electron-phonon interaction. The attenuation coefficient has been written in the form $\Gamma=\Gamma_F(\omega_q/\omega_F)\Phi(\omega_F/\omega_q)$, with $\Gamma_F=(\Gamma_q/q)(\omega_F/v_s)$, $\omega_F=\Omega|\epsilon_F/\Delta|^{2\nu/\alpha}$. (Note that Γ_q/q does not depend on frequency.) The Fermi energy is fixed to some value $\epsilon_F\ll\Delta$, and defines the smallest level spacing $\hbar\omega_F$ for extended EL's. Consequently, $\omega_q\simeq\omega_F$ marks the onset of strong SAW attenuation. For high frequencies $\omega_q\gg\omega_F$, the attenuation coefficient increases linearly with frequency. This is just the behavior predicted by the classical description of sound absorption for piezoelectric interaction; see Eq. (74) below.

For $T\ll\epsilon_\omega$, the width of the absorption region is determined by $|\epsilon_F|\simeq\epsilon_\omega$. This is merely the condition for real transitions to occur, and is not associated with the interaction vertices $\gamma_{\boldsymbol{q}}$ nor is it a consequence of the matrix element (39) whose derivation is based on the particular assumption $\nu\approx\frac{1}{2}$. We believe, therefore, that this result applies to other half-integer filling factors ν as well. To express the relation $|\epsilon_F|\simeq\epsilon_\omega$ in terms of the filling factor $\nu=2\pi l_B^2 n$, we write the electron density n as an integral over the Gaussian density of states,

$$g(\epsilon)=(2\pi)^{-3/2}(l_B^2\Delta)^{-1}\exp(-\epsilon^2/2\Delta^2), \tag{70}$$

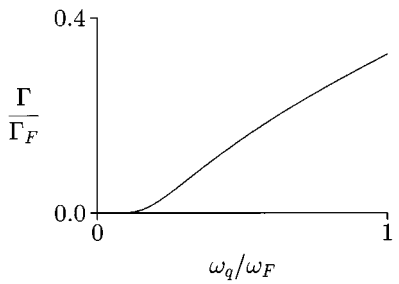

FIG. 3. The attenuation coefficient Γ, Eq. (66), as a function of the SAW frequency ω_q for a fixed Fermi energy.

and the Fermi distribution function f,

$$\overline{\nu(\epsilon_F)}=\frac{1}{\sqrt{2\pi}\Delta}\int_{-\infty}^{\infty}d\epsilon\, e^{-\epsilon^2/2\Delta^2}f(\epsilon-\epsilon_F), \tag{71}$$

and expand around the center of the LL with respect to $|\epsilon_F|/\Delta\ll 1$. For $T\ll\Delta$, this gives

$$\Delta\overline{\nu(\epsilon_F)}=\overline{\nu(\epsilon_F)}-\overline{\nu(0)}=\frac{\epsilon_F}{\sqrt{2\pi}\Delta}. \tag{72}$$

Then the width of the absorption region is obtained as

$$|\Delta\overline{\nu}|\simeq\left(\frac{\omega_q}{\Omega}\right)^{\alpha/2\nu}\simeq\left(q\Lambda\frac{v_s}{\overline{v_D}}\right)^{\alpha/2\nu}. \tag{73}$$

The exponent is given by $\alpha/2\nu=\sigma/\lambda=\frac{3}{7}\approx 0.42$. This value agrees with the exponent κ which determines the shrinking of the peaks in the longitudinal conductivity[32,15] σ_{xx} as the temperature T goes to zero, $|\Delta\overline{\nu}|\sim T^{\kappa}$. In our case the broadening of the absorption peak arises from the frequency ω_q. In this sense, $\hbar\omega_q$ may be considered as an effective temperature which replaces the real temperature T. Frequency scaling in the integer quantum Hall regime has been observed in microwave experiments.[33] For spin-split LL's, the width of the peaks in $\mathrm{Re}\sigma_{xx}$ corresponding to different LL's was found to scale as $|\Delta\overline{\nu}|\sim\omega^{\kappa}$, with $\kappa\approx 0.41$.

Due to the drift velocity $\overline{v_D}$, the width (73) depends weakly on the absolute value of the magnetic field. In terms of the filling factor, Eq. (73) can be written in the form $|\Delta\overline{\nu}|\approx(n\Lambda^2\hbar\omega_q/\Delta)^{\alpha/2\nu}(\overline{\nu})^{-\alpha/2\nu}$. Thus, $|\Delta\overline{\nu}|$ is smaller for higher (half-integer) filling factors $\overline{\nu}$. The width of the absorption region scales with the phonon wave vector as $|\Delta\overline{\nu}|\sim q^{\alpha/2\nu}$. In contrast, in the fractional quantum Hall regime, the width increases linearly with q for $\overline{\nu}=\frac{1}{2}$. This linear dependence is derived within the composite fermion model[14] and is well confirmed experimentally[8,9].

The absorption of SAW's in the integer quantum Hall regime has also been studied in Ref. 15. These authors first determine the ac conductivity of the 2DEG, which is then related to the attenuation coefficient using the equation

$$\Gamma=\frac{1}{2}K_{\mathrm{eff}}^2\frac{q\sigma'}{(1+\sigma'')^2+(\sigma')^2}, \tag{74}$$

where K_{eff}^2 represents the effective piezoelectric coupling constant [$=6.4\times10^{-4}$ for GaAs (Ref. 5)] and $\sigma'=\mathrm{Re}\sigma_{xx}(\omega_q,q)/\sigma_M$, $\sigma''=\mathrm{Im}\sigma_{xx}(\omega_q,q)/\sigma_M$, and $\sigma_M=v_s\overline{\varepsilon}/2\pi$. [Note that Eq. (74) can be obtained from Eq. (66) writing the dielectric function of the 2DEG in the form $\varepsilon(\omega,q)=1+i\sigma_{xx}(\omega_q,q)/\sigma_M$.] Assuming that $|\sigma_{xx}|\ll\sigma_M$ for sufficiently high frequencies,[15] Eq. (74) reduces to $\Gamma(\omega_q,q)\sim q\ \mathrm{Re}\sigma_{xx}(\omega_q,q)$. That is, in this case, the sound absorption and the longitudinal conductivity are related such that the width and the shape of their peaks as function of $\overline{\nu}$ are identical. The calculation of the ac conductivity in Ref. 15 is based on the concept of variable-range hopping between pairs of localized states. For $\hbar\omega_q\gg T$, the absorption of SAW's is due to resonant phononless transitions of the electrons from one site of a pair to the other. This mechanism is strongly affected by the electron-electron interaction.[15] The width of the absorption peak at half-integer filling factors was found to be

$$|\Delta\overline{\nu}|\simeq(q\xi_0)^{1/\gamma}, \tag{75}$$

where $\gamma\approx 2.3$ is the scaling exponent of the localization length

$$\xi\simeq\xi_0|\overline{\nu}-\overline{\nu(0)}|^{-\gamma}, \tag{76}$$

and ξ_0 is assumed to be of the order of the magnetic length. [Note the differences between the last equation and the semiclassical definition of the localization length in Eq. (31).] The result of Ref. 15, Eq. (75), agrees with our result, Eq. (73), in both the numerical value of the exponent and the dependence on q. However, the width $|\Delta\overline{\nu}|$ in Eq. (75) exhibits a different dependence on the magnetic field, namely, $|\Delta\overline{\nu}|\sim B^{-1/2\gamma}$, in contrast to $|\Delta\overline{\nu}|\sim B^{\alpha/2\nu}$ predicted by Eq. (73). The authors of Ref. 15 did not give a definite description of the shape of the absorption peak, but rather suggested two scenarios which eventually lead to a flat peak with a broad maximum or a double peak, respectively. Our results support the latter one; see Fig. 2.

VII. SUMMARY

We have calculated the dielectric function $\varepsilon(\omega,q)$ and the attenuation coefficient Γ of a surface acoustic wave for a 2DEG in a smooth random potential (with amplitude Δ and correlation length Λ) and a strong magnetic field corresponding to a filling factor $\overline{\nu}$ close to $\frac{1}{2}$. Both quantities become independent of temperature as the temperature is reduced below a frequency-dependent value $\epsilon_\omega=\Delta(\omega/\Omega)^{\alpha/2\nu}$, where $\alpha/2\nu=\frac{3}{7}$, $\Omega=2\pi\overline{v_D}/\Lambda$, and $\overline{v_D}$ is the average drift velocity of the electrons on the equipotential lines of the random potential. In this low-temperature, high-frequency regime (e.g., $\epsilon_\omega\simeq 1\mathrm{K}$ for $\omega=2\pi\times 100$ MHz), Im $\varepsilon(\omega,q)$ and Γ are only appreciable when ϵ_F is within a narrow region around the center of the Landau level, and Re $\varepsilon(\omega,q)$ decreases according to a power law with increasing distance from the center. In particular, the attenuation of the SAW is exponentially small except for a region whose width $|\Delta\overline{\nu}|\sim\omega^{\alpha/2\nu}$. This scaling is nonuniversal because $|\Delta\overline{\nu}|$ depends on the absolute value of the magnetic field; see Eq. (73). The dependence of Γ on the Fermi energy (or the filling factor) yields a double peak which is centered at the filling factor $\overline{\nu}=\frac{1}{2}$; cf. Fig. 2. The minimum of the absorption at $\overline{\nu}=\frac{1}{2}$ results from the enhanced screening due to the 2DEG, i.e., from the large magnitude of the dielectric function $|\varepsilon(\omega_q,q)|\simeq e^2/\overline{\varepsilon}v_s\hbar$, where $\overline{\varepsilon}$ is the average of the dielectric constants of GaAs and vacuum, and v_s is the sound velocity. The double peak in Γ is most pronounced for an infinite

system where the critical diameter $\mathcal{D}_c$, Eq. (31), of the equipotential lines of the random potential is allowed to take on arbitrarily large values. A real system of size L restricts the diameter to $\mathcal{D}_c \lesssim L$, resulting in an increase of the attenuation coefficient near the center of the Landau level. While this effect is weak for a macroscopic sample size, a similar but more pronounced effect may arise from a nonuniform electron density associated with a spatially varying filling factor.

In the high-temperature, low-frequency regime, the dielectric function decreases with rising temperature, leading to an increase of the magnitude of the attenuation coefficient and a significant increase of the width of the absorption region around $\overline{\nu} = \frac{1}{2}$.

ACKNOWLEDGMENTS

Financial support by the German-Israeli Foundation is gratefully acknowledged. We thank J. Hajdu and D. Polyakov for valuable discussions and comments. One of us (A.K.) thanks the Deutsche Forschungsgemeinschaft for financial support and B. Zingermann for a discussion of some properties of Gaussian distributions.

[1] G. W. Farnell, in *Acoustic Surface Waves*, edited by A. A. Oliner (Springer, Berlin, 1978).
[2] A. Mayer, Phys. Rep. **256**, 237 (1995).
[3] V. W. Rampton, K. McEnaney, A. G. Kozorezov, P. J. A. Carter, C. D. W. Wilkinson, M. Henin, and O. H. Hughe, Semicond. Sci. Technol. **7**, 641 (1992).
[4] A. Wixforth, J. P. Kotthaus, and G. Weimann, Phys. Rev. Lett. **56**, 2104 (1986).
[5] A. Wixforth, J. Schriba, M. Wassermeier, J. P. Kotthaus, G. Weimann, and W. Schlapp, Phys. Rev. B **40**, 7874 (1989).
[6] A. Schenstrom, Y. J. Qian, M. F. Xu, H. P. Baum, M. Levy, and B. K. Sarma, Solid State Commun. **65**, 739 (1988).
[7] A. Esslinger, R. W. Winkler, C. Rocke, A. Wixforth, J. P. Kotthaus, H. Nickel, W. Schlapp, and R. Lösch, Surf. Sci. **305**, 83 (1994).
[8] R. L. Willet, M. A. Paalanen, R. R. Ruel, K. W. West, L. N. Pfeiffer, and D. J. Bishop, Phys. Rev. Lett. **65**, 112 (1990).
[9] R. L. Willet, Surf. Sci. **305**, 76 (1994).
[10] J. M. Shilton, D. R. Mace, V. I. Talyanskii, M. Y. Simmons, M. Pepper, A. C. Churchill, and D. A. Ritchie, J. Phys. Condens. Matter **7**, 7675 (1995).
[11] J. H. McFee, in *Physical Acoustics*, edited by W. P. Mason (Academic, London, 1966), Vol. 4A.
[12] J. W. Tucker and V. W. Rampton, *Microwave Ultrasonics in Solid State Physics* (North-Holland, Amsterdam, 1972).
[13] M. Janßen, O. Viehweger, U. Fastenrath, and J. Hajdu, *Introduction to the Theory of the Integer Quantum Hall Effect* (VCH, Weinheim, 1994).
[14] B. I. Halperin, P. A. Lee, and N. Read, Phys. Rev. B **47**, 7312 (1993).
[15] I. L. Aleiner and B. I. Shklovskii, Int. J. Mod. Phys. B **8**, 801 (1994).
[16] H. L. Zhao and S. Feng, Phys. Rev. Lett. **70**, 4134 (1993).
[17] O. Heinonen, P. L. Taylor, and S. M. Girvin, Phys. Rev. B **30**, 3016 (1984).
[18] S. Iordansky and Y. B. Levinson, Phys. Rev. B **35**, 7308 (1996).
[19] S. M. Badalyan and Y. B. Levinson, Fiz. Tverd. Tela (Leningrad) **30**, 2764 (1988) [Sov. Phys. Solid State **30**, 1592 (1988)].
[20] L. D. Landau and E. M. Lifschitz, *Theory of Elasticity* (Pergamon, Oxford, 1970), Vol. 7.
[21] S. H. Simon (unpublished).
[22] V. F. Gantmakher and Y. B. Levinson, *Carrier Scattering in Metals and Semiconductors* (North-Holland, Amsterdam, 1987).
[23] F. Guillion, A. Sachrajda, M. D'Iorio, R. Boulet, and P. Coleridge, Can. J. Phys. **69**, 461 (1991).
[24] S. A. Trugman, Phys. Rev. B **27**, 7539 (1983).
[25] H. A. Fertig and B. I. Halperin, Phys. Rev. B **36**, 7969 (1987).
[26] R. Mehr and A. Aharony, Phys. Rev. B **37**, 6349 (1988).
[27] D. Stauffer and A. Aharony, *Introduction to Percolation Theory* (Taylor and Francis, London, 1992).
[28] T. Grossman and A. Aharony, J. Phys. A **19**, L745 (1986).
[29] M. S. Longuet-Higgins, Philos. Trans. R. Soc. London Ser. A **249**, 321 (1957).
[30] M. B. Isichenko, Rev. Mod. Phys. **64**, 961 (1992).
[31] U. Wulf, V. Gudmundsson, and R. R. Gerhardts, Phys. Rev. B **38**, 4218 (1988).
[32] H. P. Wei, Y. Lin, D. C. Tsui, and A. M. M. Pruisken, Phys. Rev. B **45**, 3926 (1992).
[33] L. W. Engel, D. Shahar, C. Kurdak, and D. C. Tsui, Phys. Rev. Lett. **71**, 2638 (1993).